Article

Chinese Science Bulletin

Progress of Projects Supported by NSFC
Materials Science

February 2012 Vol.57 No.5: 435–444
doi: 10.1007/s11434-011-4914-0

Restoration of rat calvarial defects by poly(lactide-co-glycolide)/ hydroxyapatite scaffolds loaded with bone mesenchymal stem cells and DNA complexes

LI Dan[1,2], WANG Wei[1], GUO Rui[1], QI YiYing[3], GOU ZhongRu[2] & GAO ChangYou[1,4*]

[1] *Key Laboratory of Macromolecular Synthesis and Functionalization of Ministry of Education, Department of Polymer Science and Engineering, Zhejiang University, Hangzhou 310027, China;*
[2] *Zhejiang-California International NanoSystems Institute, Hangzhou 310027, China;*
[3] *Department of Orthopedic Surgery, Second Affiliated Hospital, Zhejiang University, Hangzhou 310027, China;*
[4] *State Key Laboratory of Diagnosis and Treatment for Infectious Diseases, First Affiliated Hospital, College of Medicine, Zhejiang University, Hangzhou 310003, China*

Received September 3, 2011; accepted November 3, 2011; published online December 16, 2011

A composite construct comprising of a bone mesenchymal stem cell (BMSC) sheet, plasmid DNA, encoding human bone morphogenic protein-2 (hBMP-2), and poly(lactide-co-glycolide)/hydroxyapatite (PLGA/HA) sponge was designed and employed in the restoration of rat calvarial defects. To improve gene transfection efficiency, a cationic chitosan derivative, *N*,*N*,*N*,-trimethyl chitosan chloride (TMC), was employed as the vector. The TMC/DNA complexes had a transfection efficiency of 13% in rat BMSCs, resulting in heterogeneous hBMP-2 expression in a 10-d culture period *in vitro*. *In vivo* culture of the composite constructs was performed by implantation into rat full-thickness calvarial defects, using constructs lacking pDNA-hBMP-2 or BMSC sheets as controls. Significantly higher heterogeneous expression of hBMP-2 was detected *in vivo* at 2 weeks for the cell sheet/DNA complex/scaffold constructs, compared with the constructs lacking pDNA-hBMP-2 or BMSC sheets. New bone formation was evident as early as 4 weeks in the experimental constructs. At 8 weeks, partial bridging of calvarial defects was observed in the experimental constructs, which was significantly better than the constructs lacking pDNA-hBMP-2 or BMSC sheets. Therefore, the combination of the PLGA/HA scaffold with BMSC sheets and gene therapy vectors is effective at enhancing bone formation.

gene therapy, bone regeneration, bone marrow stem cells, poly(lactide-co-glycolide), BMP-2

Citation: Li D, Wang W, Guo R, et al. Restoration of rat calvarial defects by poly(lactide-co-glycolide)/hydroxyapatite scaffolds loaded with bone mesenchymal stem cells and DNA complexes. Chin Sci Bull, 2012, 57: 435–444, doi: 10.1007/s11434-011-4914-0

Bone regeneration is one of the hot topics of research in the field of regenerative medicine. Many strategies have been investigated in bone tissue engineering, including cell-based strategies, scaffold development and growth factor delivery. The combination of regenerative medicine and gene therapy offers new opportunities to target multiple factors at once, which may help increase the potential of these techniques for promoting bone repair.

Numerous growth factors currently used in bone tissue engineering, including bone morphogenic protein-2 (BMP-2), which is well-known for its powerful ability to commit mesenchymal stem cells (MSCs) towards an osteogenic lineage and induce new bone formation [1]. However, a major limitation of growth factors is that they can be expensive and generally have a short-half life. Gene therapy has been investigated as an alternative method for BMP delivery and there has been some evidence that proteins synthesized endogenously as a result of gene transfection have greater biologic activities than their recombinant counterparts [2]. The general protocol for gene therapy in tissue

*Corresponding author (email: cygao@mail.hz.zj.cn)

repair is to transplant cells transfected by gene/vector complexes *in vitro* [3]. However, prolonged expression of the proteins from *in vitro* transfected cells is dependent on the survival of the transplanted cells during implantation and within the defect. An alternative protocol is to directly load the gene or gene/vector complexes into the scaffold, resulting in the seeded cells and/or endogenous cells being transfected *in situ* [4,5]. To enhance the body's innate capacity to repair bone defects after injury, composite scaffolds of polymer and ceramic particles are preferred because of their favorable mechanical properties and bioactivity [6,7]. Previously, we have developed a poly(lactide-co-glycolide) (PLGA) scaffold with hydroxyapatite nanoparticles embedded in the pore walls (PLGA/HA), which enhanced osteoblastic differentiation of bone marrow stem cells (BMSCs) *in vitro* [8].

Compared with the traditional method of directly seeding cells in scaffolds, the cell sheet technique makes it possible to deliver a much larger number of cells for efficient tissue regeneration [9]. The cell sheet can be easily detached from the culture substrate using a cell-scraper, which enables the extracellular matrix and cell-cell interactions to remain intact as no enzymatic treatments are used. Recent studies have shown that the cell sheet technique is effective for the treatment of myocardial infarction [10], tendon defects [9] and periodontitis [11]. The cell sheet technique contributes to bone formation in cases of osseointegration [12], nonunion [13], various bone defects [14,15] and spinal interbody fusion [16].

To the best of our knowledge, there is no report on the fabrication of a composite construct integrated with a PLGA/HA scaffold, BMSC sheet and gene therapy for bone regeneration. The aim of this study is to evaluate the feasibility of this method for bone formation in rat calvarial defect models.

1 Materials and methods

1.1 Materials

Poly(lactide-co-glycolide) (PLGA, 75/25 lactide/glycolide ratio, M_n=78.5 kD, M_w=132.4 kD) was purchased from China Textile Academy. Paraffin (melting point, 53–56°C), 1,4-dioxane and hexane were obtained from Shanghai Chemical Industries Co., Ltd. Dulbecco's modified Eagle's medium (DMEM) and fetal bovine serum (FBS) were obtained from GIBCO (Life Technologies, Grand Island, New York, USA). Quant-iT™ PicoGreen dsDNA reagent (an intercalating fluorescent dye) was purchased from Invitrogen (Life Technologies). Hochest 33258 and methyl tetrazolium (MTT) were obtained from Sigma (Sigma-Aldrich, St. Louis, MO, USA). Millipore water was used throughout the study. All other reagents were of analytical grade and used as received.

1.2 Cell culture and cell sheet preparation

Bone marrow stem cells (BMSCs) were isolated from the bone marrow of young adult male Sprague-Dawley rats as previously described [17]. The procedures were performed in accordance with the "Guidelines for Animal Experimentation" by the Institutional Animal Care and Use Committee, Zhejiang University. Briefly, bone marrow cells were obtained from the femoral shafts of rats by flushing out with 10 mL of culture medium (low glucose DMEM supplemented with 10% FBS, 100 μg/mL penicillin and 100 U/mL streptomycin). The released cells were collected in two flasks (75-cm^2 culture flask, Corning Inc., USA) containing 15 mL culture medium and incubated in a humidified atmosphere of 95% air with 5% CO_2 at 37°C. After reaching about 80% confluency, cells were detached and serially subcultured. BMSCs at passage 2 (P2) were used in this study.

To prepare the cell sheet, BMSCs of P2 were harvested, reseeded in flasks (25-cm^2 culture flask, Corning Inc.), and cultured in low-glucose DMEM with 10% FBS for about two weeks without passaging. The culture medium was changed every 2 d. BMSC sheets formed spontaneously and could be detached intact from the substrate using a cell-scraper (Figure 1(a)). About 4.6×10^6 cells were contained within a single cell sheet, as determined by DNA quantification using a fluorometer (LS55, Perkin-Elmer, Waltham, MA, USA) with the fluorescent dye Hoechst 33258 [18].

1.3 Preparation of TMC/DNA complexes

N,*N*,*N*-trimethyl chitosan chloride (TMC) was synthesized according to the previously reported method [19]. The chemical structure of the product was characterized by ^{1}H NMR spectroscopy (300 MHz, Varian, Agilent Technologies, Santa Clara, CA, USA). The chemical shifts with peak positions at δ 3.2 and 2.0 were assigned to $-N(CH_3)^{3+}$ and $-COCH_3$, respectively, according to which the degree of quaternization was determined to be 38%.

TMC and DNA were dissolved in Millipore water to obtain 1 mg/mL solutions, which were filtered through syringe filters (Durapore, Millipore, Billerica, MA, USA) with a pore size of 0.22 μm for sterilization. The TMC solution was added to the DNA solution and vortexed vigorously for 30 s, and further incubated for 30 min at 37°C before use or characterization. The N/P ratio (molar ratio of amine groups to phosphate groups) used in this study was fixed at 10, as TMC/DNA complexes of this ratio have the highest transfection efficiency *in vitro* [19]. The morphology and the mean diameter of the TMC/DNA complexes were characterized by scanning electron microscopy (SEM, JEOL JEM-200CX, Tokyo, Japan).

1.4 *In vitro* cytotoxicity and gene transfection evaluation

The cytotoxicity of different concentrations of TMC/DNA

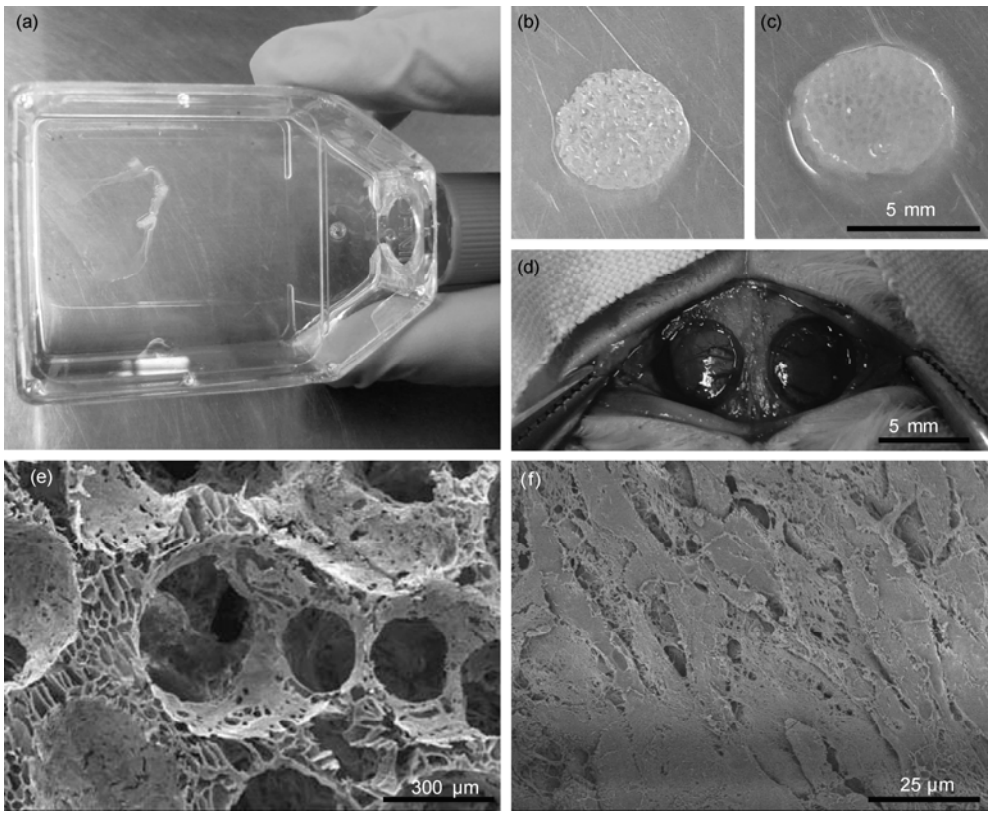

Figure 1 Macroscopic images of (a) BMSC sheet, (b) PLGA/HA scaffold, (c) PLGA/HA/pDNA complexes/cell sheet construct, and (d) rat calvarial defects with a diameter of 5 mm. SEM images of (e) PLGA/HA scaffold, and (f) PLGA/HA scaffold wrapped in a BMSC sheet.

complexes was evaluated via MTT assay [19]. Briefly, BMSCs were seeded in a 96-well plate at a concentration of 5×10^3 cells per well and cultured overnight. The culture medium was then removed and 100 μL DMEM/10% FBS containing 10 μg naked DNA or TMC/DNA particles with normalized DNA concentrations of 0.2, 2 or 10 μg per 10^4 BMSCs were added to each well. BMSCs cultured in normal DMEM/10% FBS medium without DNA were used as a control. The culture medium was exchanged with the corresponding medium for each of the groups every 2 d throughout the culture period. Each value was averaged from three parallel experiments.

The transfection efficiency was determined by 2D culture using pDNA-eGFP. Briefly, 5×10^4 BMSCs were seeded into each well of a 12-well culture plate and cultured overnight. After the culture medium was removed, the TMC/pDNA-eGFP complexes (2 μg DNA per 10^4 BMSCs) were added with DMEM. Eight hours later, the culture medium was exchanged with DMEM containing FBS. The cells were detached from the plate after 3 d and characterized by flow cytometry (FACS, FACSCalibur, BD Bioscience, Franklin Lakes, NJ, USA).

The extent of hBMP-2 expression *in vitro* was determined using pDNA-hBMP-2, rather than pDNA-eGFP, and quantified using an ELISA kit (RapidBio, West Hills, CA, USA), following the manufacturer's instructions. The cell density was determined by DNA quantification using a fluorometer (LS55, Perkin-Elmer) with the fluorescent dye Hoechst 33258 [18]. After correlating the DNA quantity with the cell number by a standard curve, the average hBMP-2 expression level per 10^5 cells was calculated. All data were averaged from three parallel measurements.

1.5 Preparation of DNA-loaded PLGA/HA Scaffolds

PLGA/HA Scaffolds were fabricated by a porogen-leaching method as previously described [8]. Briefly, the HA nanoparticle-coated paraffin spheres were prepared via Pickering emulsion. The sieved HA-coated paraffin spheres (450–600 μm) were added into a Teflon mold, which was incubated in an oven at 45°C for 30 min to bind the spheres. After cooling to room temperature, around 1 mL 12% PLGA/1,4-dioxane solution was cast dropwise onto the HA-coated paraffin sphere assembly. The system was subsequently frozen at –25°C for 2 h and then freeze-dried to remove the 1,4-dioxane. The PLGA/HA porous scaffolds were finally obtained by leaching the paraffin assembly in 400 mL hexane at 37°C for 2 d, changing the hexane every 4 h. To observe the inner microstructure under SEM, the porous scaffolds were fractured in liquid nitrogen. The porosity of the scaffolds was determined by ethanol inhalation [20].

PLGA/HA scaffolds, with an average diameter of 5 mm and a height of 1 mm (Figure 1(b)), were sterilized with 75 vol% ethanol for 4 h and incubated in phosphate-buffered

saline (PBS) for 1 d to exchange the ethanol solution. TMC/DNA complex solution (0.2 mg/mL DNA) was used to fill the pores of the scaffolds, which were then kept at 4°C overnight and freeze-dried to facilitate the complete incorporation of the TMC/DNA complexes.

Each PLGA/HA scaffold containing TMC/DNA complexes was immersed in 0.5 mL of 25 mg/mL papain/PBS solution containing 4 mg/mL EDTA and digested overnight at 60°C. The total loaded amount of DNA on the scaffolds was assessed by fluorometry (LS55, Perkin-Elmer) using PicoGreen at excitation and emission wavelengths of 480 and 520 nm, respectively. An *in vitro* release assay was conducted to determine the release kinetics of DNA from the PLGA/HA scaffolds. Each of the PLGA/HA scaffolds containing the TMC/DNA complexes was immersed in 1 mL of sterile PBS and gently stirred at 37°C. At desired time intervals, 0.2 mL of the supernatant was collected for analysis and replaced with an equal volume of fresh PBS. The 0.2 mL supernatant was added into 0.3 mL of 25 mg/mL papain/PBS solution containing 4 mg/mL EDTA and digested overnight at 60°C. The quantity of the released DNA was analyzed by fluorometry with PicoGreen. All data were averaged from three parallel measurements and expressed as mean ± standard deviation (SD).

1.6 Surgical procedures

To prepare the implants, the BMSC sheet was wrapped around the scaffold with or without the incorporation of TMC/DNA complexes. The implants were divided into three groups as follows:

Group A, PLGA/HA/(TMC/pDNA-hBMP-2 complexes)/cell sheet; $n = 18$;

Group B, PLGA/HA/cell sheet; $n = 16$;

Group C, PLGA/HA/(TMC/pDNA-hBMP-2 complexes); $n = 18$.

Three samples from each group were used to study the *in vivo* expression of hBMP-2 in rat calvarial defects after 2 weeks of implantation by qRT-PCR. Another 3 samples from each group were used for micro-computed tomography after 8 weeks of implantation and were subsequently used for hematoxylin and eosin (H&E) staining. A total of 5 samples from each group were used for H&E staining after implantation for 4 and 8 weeks, respectively. Three samples in each group were used for analysis of gene expression in repaired tissues after 8 weeks of implantation.

Twenty-five 12–13-week-old male Sprague-Dawley rats (250–300 g) were housed in a light- and temperature-controlled environment, with free access to food and water. The rats were anaesthetized by injection of ketamine hydrochloride (3.5 mg/kg of body weight; China National Medicines Corporation Ltd, Beijing, China) into the peritoneal cavity. For the calvarial defect model, the dorsal part of the cranium was shaved and a linear incision of approximately 20 mm was opened over the scalp of each animal. The periosteum was removed and two full-thickness calvarial defects were prepared (5 mm in diameter) in the parietal bone using a slow speed dental drill (Figure 1(d)). Constant saline irrigation was performed and the dura mater was kept intact during the procedure. After placement of the constructs into the defects, the skin was sutured.

1.7 Micro-computed tomography (μCT) and histology

The rats were euthanized after implantation for 4 or 8 weeks. Block samples, including the surgical sites, were harvested and fixed in 4% paraformaldehyde at 37°C for 48 h. Three samples at 8 weeks from each group were scanned using a micro-CT system (Explore Locus; GE Healthcare, Chalfont St. Giles, Buckinghamshire, UK) in a high-resolution scanning mode (voxel size and slice thickness of 45 μm). Three-dimensional images were reconstructed, and the volume of the regenerated bone within the defects was calculated using the auxiliary software, MicroVIEW (GE Healthcare).

For histological examination, samples were decalcified in 10% EDTA for 3 weeks at room temperature, dehydrated using an ascending alcohol gradient and embedded in paraffin. Longitudinal sections were stained with H&E and visualized using an optical microscope (DXM200F Digital Camera; Nikon, Tokyo, Japan). Five defects per group were analyzed at each time point.

1.8 Quantitative reverse transcription-polymerase chain reaction (qRT-PCR)

In vivo expression of hBMP-2 was determined by qRT-PCR in rat calvarial defects two weeks post-implantation and in repaired tissues at 8 weeks. Three samples were used for each assay (n=3). Total RNA was extracted using the RNeasy Mini Kit (Qiagen, Montgomery, AL, USA) and ~1 μg of total RNA was used for reverse-transcription into cDNA with the Omniscript RT Kit (Qiagen). QRT-PCR of hBMP-2, type I collagen (COL I) and osteocalcin (OCN) was performed in an ABI 7300 real-time PCR system (Applied Biosystems, Life Technologies) with SYBR Green PCR master mix (Applied Biosystems), under the following conditions: 15 s at 90°C, 60 s at 60°C, with the fluorescence intensity being recorded for 40 cycles. C_T (threshold cycle) values were calculated using the iQ5 optical system software (Version 2, Bio-Rad, Berkeley, CA, USA). The mathematical model previously described in detail was used to determine the expression ratio of genes [21]. Primer sequences used in quantitative real-time PCR were GAPDH sense, 5′-GGTGGACCTCATGGCCTACAT-3′; GAPDH antisense, 5′-GCCTCTCTCTTGCTCTCAGTATCCT-3′; hBMP-2 sense, 5′-CCAAGATGAACACAGCTGGTCACAGA-3′; hBMP-2 antisense, 5′-CCCACGTCACTGAAGTCCACG-3′; Rat collagen I sense, 5′-ACCTCCGGCTCCTGCTCCTCTTAG-3′; Rat collagen I antisense, 5′-GACA-

GCACTCGCCCTCCCGTTTTT-3′; Rat Osteocalcin sense, 5′-CTCACTCTGCTGGCCCTGAC-3′; Rat Osteocalcin antisense, 5′-CACCTTACTGCCCTCCTGCTTG-3′.

1.9 Statistics

Data are expressed as mean ± SD. Statistical analysis was performed by two-tailed Student's *t*-tests between two groups. All statistical computations were performed using SPSS version 16.0 (SPSS Inc., Chicago, IL, USA). $P < 0.05$ was considered statistically significant.

2 Results

2.1 Properties of the composite construct

The BMSC sheet could be detached intact with a cell-scraper as depicted in Figure 1(a), and wrapped tightly around the PLGA/HA scaffold loaded with DNA/TMC complexes (Figure 1(c)). The PLGA/HA sponges (Figure 1(b),(e)) used in this work were prepared by a porogen-leaching method using HA-coated paraffin spheres of 450–600 μm diameter as the porogen. As the average pore size was larger than 450 μm, the porosity measured by ethanol inhalation was ~90%. Their size matched exactly the size of the calvarial defects (Figure 1(d)). By comparison with the pristine sponge (Figure 1(e)), the cell sheet wrapping resulted in dense and uniform cells on the construct surface (Figure 1(f)).

As shown in Figure 2(a), the positively-charged TMC could effectively condense the negatively-charged DNA and yield small particles with an average diameter of ~100 nm, as detected by SEM in a dry state. All the complexes were well dispersed with a typical spherical morphology.

The cell viability of rat BMSCs exposed to different concentrations of TMC/DNA complexes or naked DNA was evaluated by MTT assay (Figure 2(b)). For direct comparison, the OD values measured from the TMC/DNA or naked DNA samples were normalized to those of the control samples (cells cultured in normal DMEM/10% FBS medium). When the concentration of TMC/DNA complexes was lower (e.g. 0.2 μg DNA per 10^4 BMSCs), the cell viability increased during culture and was significantly larger than that of the control sample at day 7 ($P < 0.05$). Cytotoxicity was apparent at higher TMC/DNA concentrations, with cell viability decreasing to around 1/4 of the control sample at day 7 when the DNA concentration was increased to 10 μg DNA per 10^4 BMSCs. By contrast, cells cultured in medium containing naked DNA (10 μg DNA per 10^4 BMSCs) showed comparable viability to that of the control at day 7, indicating that the naked DNA is not cytotoxic. Considering the balance between the efficacy and cytotoxicity, an intermediate concentration (2 μg DNA per 10^4 BMSCs) of TMC/DNA complexes was used for the later studies.

TMC/pDNA-eGFP complexes were co-cultured with BMSCs in a 2D culture system. FACS was used to calculate the percentage of cells which expressed GFP and the mean fluorescence intensity. Figure 3(a) shows fluorescence intensity increasing from 6 to 17 after transfection. Considering that cells with relative fluorescence intensity higher than 10 are regarded as GFP-transfected cells, the gene transfection efficiency detected by FCM was ~13%. Following this, BMSCs were transfected with pDNA-hBMP-2/TMC complexes to detect growth factor production. As shown in Figure 3(b), BMSCs could effectively express hBMP-2 after transfection, with the concentration in the supernatant increasing only slightly during the experimental period until the longest determined time-point (10 d).

Each PLGA/HA scaffold adsorbed 2 μg of DNA. Figure 4 shows that the DNA was released rapidly during the first 4 h, with ~74% being released in this period. However, the residual DNA was released at a much slower rate until 72 h, by which almost all DNA was released. These results

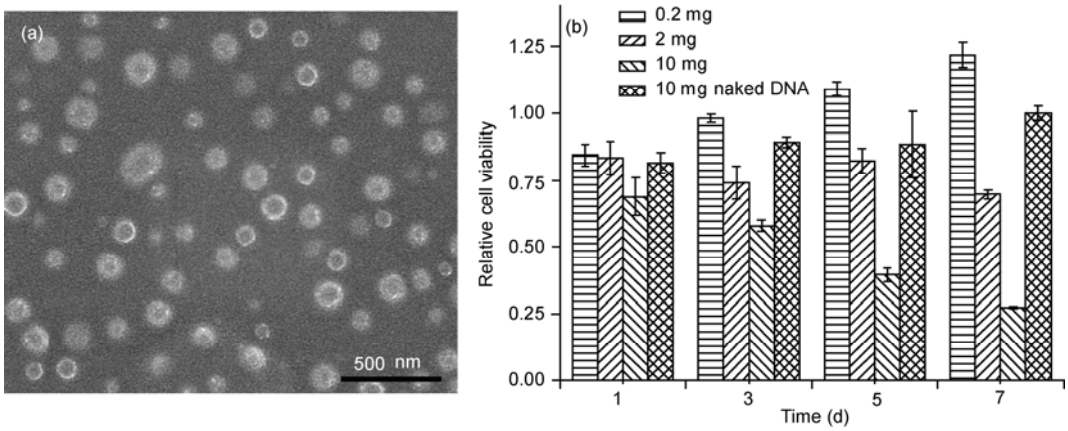

Figure 2 (a) SEM image of TMC/DNA complexes. (b) BMSC viability as a function of culture time. TMC/DNA complexes with a fixed N/P ratio of 10 or naked DNA were added to the culture medium with different concentrations of DNA (0.2, 2 and 10 μg per 10^4 BMSCs). The viability was normalized to that of control samples without DNA.

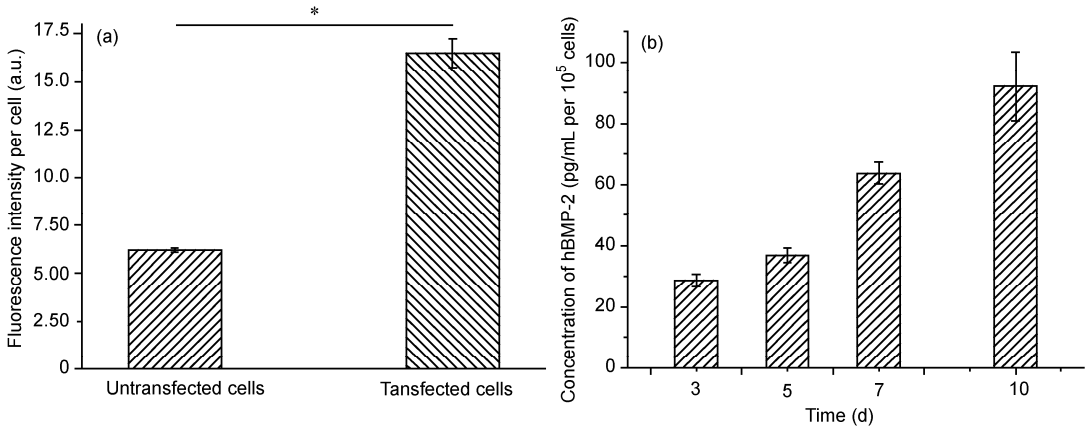

Figure 3 (a) Average fluorescence intensity of BMSCs before and after transfection with the TMC/plasmid DNA-eGFP complexes *in vitro* (2 μg plasmid DNA-eGFP per 10^4 BMSCs). Data were obtained by flow cytometry. *, $P < 0.05$. (b) *In vitro* hBMP-2 expression in the supernatant after transfection with TMC/pDNA-hBMP-2 complexes.

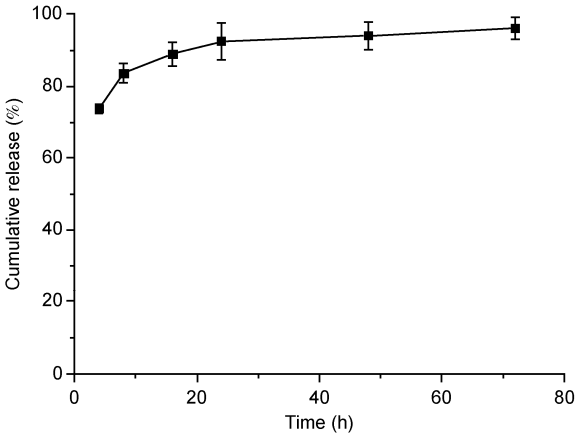

Figure 4 Cumulative released amount of DNA (TMC/DNA complexes, *N*/*P*=10) from PLGA/HA scaffold as a function of incubation time.

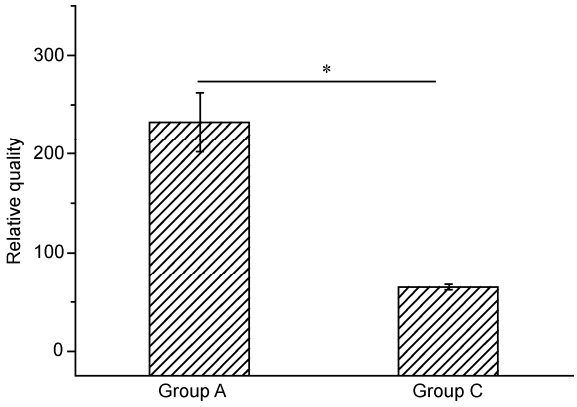

Figure 5 *In vivo* expression of hBMP-2 in rat calvarial defects for 2 weeks evaluated by qRT-PCR. Group A, PLGA/HA/(TMC/pDNA-hBMP-2 complexes)/cell sheet; Group C, PLGA/HA/(TMC/pDNA-hBMP-2 complexes). The gene expression level was normalized to that of the respective GAPDH expression. *, $P < 0.05$.

demonstrate that the DNA complexes could be easily released from the scaffold, which is as expected as only weak physical interactions exist. However, the *in vivo* release pattern, in particular after the stem cell entrapment, should be different because of the physical confinement of host tissues.

2.2 *In vivo* hBMP-2 expression

As the pDNA-hBMP-2 used in this study originated from human, it can effectively avoid the interference of host proteins produced by the rat. QRT-PCR analysis of hBMP-2 expression in the defects demonstrated that much more hBMP-2 was expressed in Group A (PLGA/HA/(TMC/pDNA-hBMP-2 complexes)/cell sheet) than Group C (PLGA/HA/(TMC/pDNA-hBMP-2 complexes)) after 2 weeks of implantation (Figure 5). No hBMP-2 was detected by qRT-PCR in Group B (PLGA/HA/cell sheet).

2.3 *In vivo* bone formation

Bone formation was evident 4 weeks after implantation in Group A. The newly-formed bone (marked as B) was identified not only close to native bone but also in the centers of the defects (Figure 6(a),(d),(g)). Bone islands were also found in the centers of the defects in Group B (Figure 6(b),(e),(h)). No new bone was formed in Group C and only obvious fibrous tissue (marked as F) could be observed in the defects (Figure 6(c),(f),(i)). Residual scaffolds (marked as S) were present in the defects in all three groups (Figure 6(d)–(f)).

Bone formation was enhanced after a longer healing time in Group A, which almost bridged the calvarial defect (Figure 7(a),(d),(g)). Many osteoblasts (marked with a black arrow) were trapped in the lacunae, and the new bone showed a more similar morphology to the host bone. No apparent increase in new bone formation was observed in Group B at 8 weeks (Figure 7(b),(e),(h)). Fibrous tissue

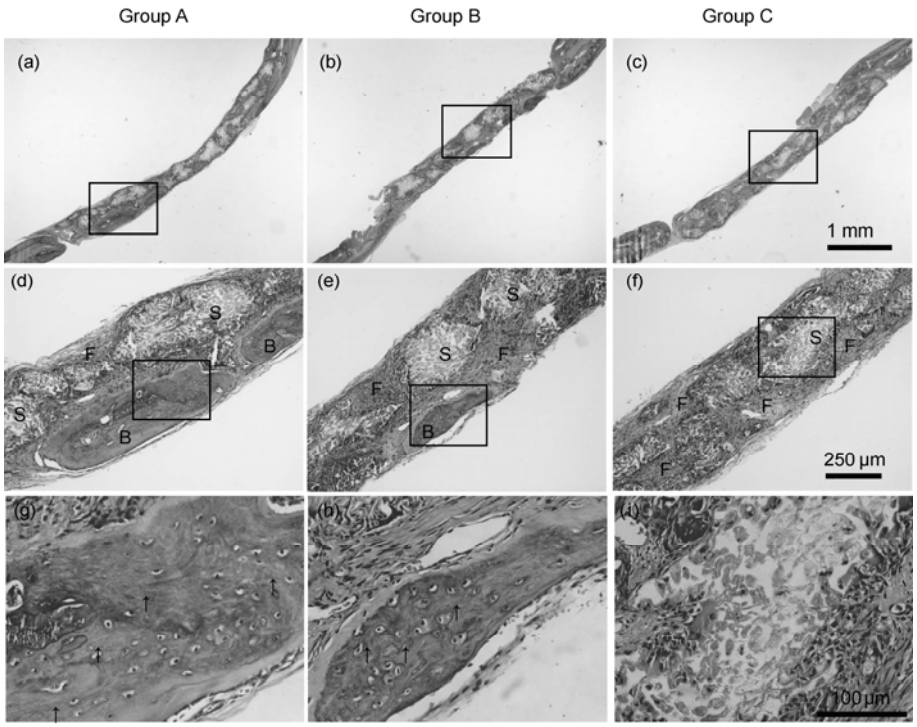

Figure 6 H&E staining photomicrographs of calvarial defect sites treated with (a, d, g) Group A, (b, e, h) Group B, and (c, f, i) Group C for 4 weeks. B, F, S and black arrows represent new bone, fibrous tissue, residual scaffold and osteoblasts, respectively.

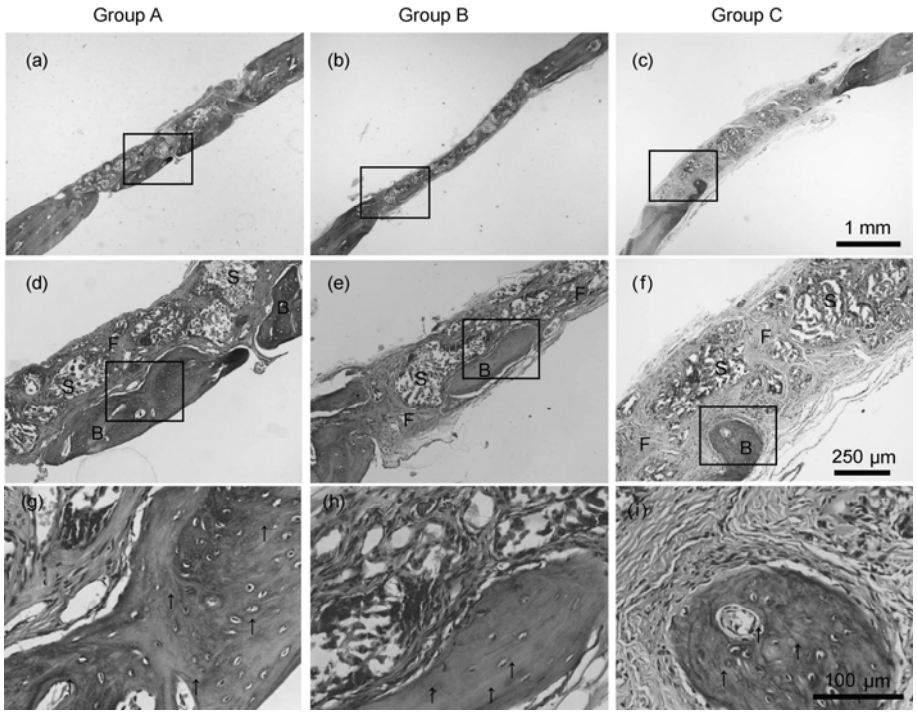

Figure 7 H&E staining photomicrographs of calvarial defect sites treated with (a, d, g) Group A, (b, e, h) Group B, and (c, f, i) Group C for 8 weeks.

became denser in Group C, and a small amount of new bone was found at the edge of the bone defect (Figure 7(c),(f), (i)). Scaffolds had been degraded significantly but were still visible (Figure 7(d)–(f)).

Micro-CT evaluations confirmed new bone formation at 8 weeks post-implantation, especially in Group A (Figure 8(a)–(c)). Bone-healing efficacy was improved in the sequence of Group C < Group B < Group A. Partial bridging was observed in Group A. Some bone islands were formed in the center of defects in Group B, but new bone was only regenerated in the periphery of defects in Group C. No complete bridging was observed in defects of all groups.

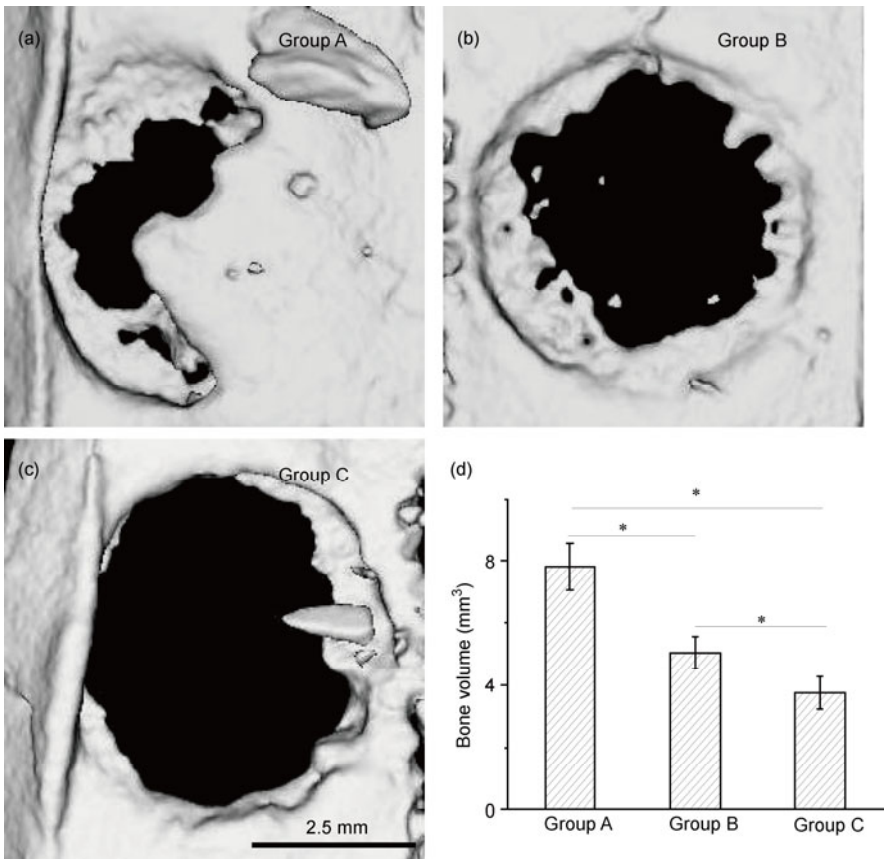

Figure 8 Representative micro-CT images of rat calvarial defects repaired by (a) Group A, (b) Group B, and (c) Group C for 8 weeks. The gray areas represent mineralized bone. (d) Quantitative bone volume analysis by micro-CT. *, $P < 0.05$.

Volumetric analysis (Figure 8(d)) showed a significantly higher volume of new bone in Group A compared with Groups B and C ($P < 0.05$). The new bone volume in Group C was around half of that in the Group A.

2.4 Analysis of gene expression

Expression of bone-related genes was analyzed by qRT-PCR (Figure 9). The level of the 2 bone special genes of the Group A was significantly higher than that of the Groups B and C ($P < 0.05$). In Group A, the expression level of collagen type I was 5- and 15-fold higher than Groups B and C, respectively. The expression level of osteocalcin in Group A was 2- and 5-fold higher than Groups B and C, respectively.

3 Discussion

It is a primary focus of orthopedic research to develop reli-

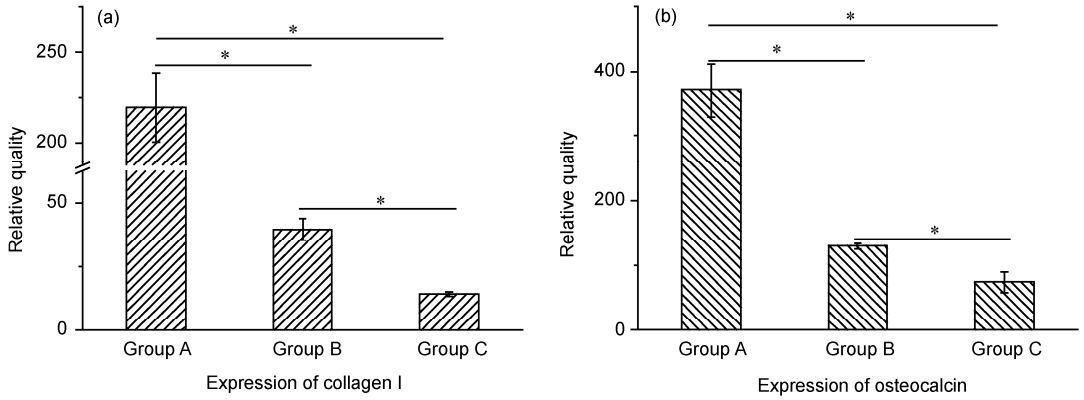

Figure 9 Gene expression profiles characterized by qRT-PCR for (a) collagen type I, and (b) osteocalcin in repaired tissues after implantation for 8 weeks. The gene expression level was normalized to that of the respective GAPDH expression. *, $P < 0.05$.

able approaches for the repair or regeneration of damaged bone [22,23]. Tissue engineering and regenerative medicine have shown great promise in promoting bone repair using MSC sheets alone or in combination with implants wrapped in MSC sheets [13,24]. Compared with the traditional method of directly seeding cells in scaffolds, the cell sheet technique makes it possible to deliver a much larger number of cells for efficient tissue regeneration [9]. As a potent regulator of cell function and differentiation, the extracellular matrix (ECM) can be well-preserved during cell sheet fabrication, thereby enhancing osteoblastic differentiation and improving bone formation [25]. Previous research demonstrates that PLGA scaffolds with a HA coating (PLGA/HA-S or PLGA/HA) have good mechanical properties and bioactivity [8]. However, PLGA/HA scaffolds are not sufficient on their own at providing instructive cues for MSC osteoblastic differentiation and new bone formation. BMP-2 is one of the most potent growth factors with a powerful ability to recruit MSCs and induce MSC osteoblastic differentiation [26,27]. Using gene therapy, recombinant BMP-2 can be expressed *in situ* after transfection with a plasmid encoding BMP-2. Therefore, in this study we fabricated a PLGA/HA scaffold, which was wrapped in a MSC sheet and complexed with gene therapy vectors, to repair rat calvarial defects with promising results.

Firstly, based on our previous results, TMC with a quaternization degree of 38% was used as the vector to condense DNA and form nano-complexes [28]. These complexes are beneficial to mask the strong negative charge of DNA and thereby facilitate uptake across the cell membrane [29]. Expression of hBMP-2 *in vitro* (Figure 3(b)) and *in vivo* (Figure 5) confirmed the success of the present gene delivery strategy.

In the animal experiments, one experimental group, Group A (PLGA/HA/(TMC/pDNA-hBMP-2 complexes)/cell sheet) and two control groups, Group B (PLGA/HA/cell sheet) without gene, and Group C (PLGA/HA/(TMC/pDNA-hBMP-2 complexes)) without BMSC sheet, were used to determine the importance of both gene therapy and BMSC sheet incorporation on bone regeneration by the present protocol. Group A showed enhanced new bone formation and up-regulation of bone-specific gene expression. This positive effect is reasonably attributed to the expression of hBMP-2 by the loaded TMC/pDNA-hBMP-2 complexes and BMSC sheet. Indeed, the expression of hBMP-2 was only detected in Groups A and C, with a significant higher level in Group A (Figure 5). Incorporation of the BMSC sheet significantly improved expression of hBMP-2; however, the BMSC sheet alone was unable to secrete detectable hBMP-2 in Group B. The BMSC sheet was previously shown to secrete larger amounts of angiogenic and antiapoptotic factors by paracrine activity [10], which may be conducive to the migration of endogenous cells. Aside from the transfection of BMSCs, hBMP-2 expression could result from the transfection of endogenous cells, such as fibroblasts, which could then produce hBMP-2 [30]. The upregulation of osteocalcin, which is a terminal marker of osteoblastic differentiation, indicates the enhanced osteoblastic differentiation of BMSC sheets in Group A.

We believe that the intrinsic mechanism behind the more efficient repair seen in the experimental group depends on both the incorporation of gene therapy and the stem cell-sheet technology. While the BMSC sheet is necessary to rebuild the bone ECM, the differentiation of BMSCs into osteoblasts is also required and is greatly enhanced by hBMP-2 gene therapy. Comparatively, the BMSC sheet plays a more important role, as bone regeneration was observed in several small regions within the central portions of defects that were covered by the transplanted cell sheets alone [31]. Moreover, although cell labeling was not used in this research, by comparing the results between Groups A and C, it is safe to conclude that many osteoblasts in the neo-tissue of Group A are differentiated from the transplanted BMSC sheet.

The results from the *in vivo* study indicate that the loading of TMC/pDNA-hBMP-2 complexes into the PLGA/HA scaffolds is not sufficient to elicit a bone regeneration response. This is in accordance with previous studies, in which scaffolds containing plasmid DNA did not result in enhanced bone formation [32,33]. The incorporation of TMC/pDNA-hBMP-2 complexes into PLGA/HA scaffolds also resulted in decreased bone formation compared with the delivery of recombinant BMP-2 protein with this system in our previous study (unpublished work). The reasons are unclear as several factors are involved during pDNA-hBMP-2 transfection as well as bone healing processes. One reason may be the low transfection efficiency seen, which may result in only low levels of BMP-2 being produced. This amount was in the range of pg in the *in vitro* study, which is far below the μg value used in the previous study [34,35]. Thus, future studies should investigate more efficient gene vectors capable of transfecting BMCs to a higher degree.

4 Conclusion

Herein, a bioactive construct of PLGA/HA/(TMC/pDNA-hBMP-2 complexes)/cell sheet was designed and manufactured for bone regeneration; its biological performance was evaluated in a rat calvarial defect model. Gene complexes had a transfection efficiency of 13% in BMSCs *in vitro*, which expressed hBMP-2 both *in vitro* and *in vivo*. Implantation of the constructs into full-thickness rat calvarial defects with a diameter of 5 mm resulted in increased new bone formation. Osteogenic genes, such as collagen type I and osteocalcin, were also up-regulated, implying the efficient osteogenic differentiation of BMSC sheets. Moreover, some small bone islands were also observed in the center of bone defects when a construct without the hBMP-2 gene

was used. By contrast, when the BMSC sheets were used in the absence of the construct, minimal bone tissue was found in the calvarial defects. Therefore, combination of the PLGA/HA scaffold with BMSC sheets and gene therapy is more effective at restoring calvarial defects by the present method.

This work was supported by the National Natural Science Foundation of China (20934003), the Science Technology Program of Zhejiang Province (2009C14003, 2009C13020), and the National Basic Research Program of China (2011CB606203).

1 Yamamoto M, Takahashi Y, Tabata Y. Enhanced bone regeneration at a segmental bone defect by controlled release of bone morphogenetic protein-2 from a biodegradable hydrogel. Tissue Eng, 2006, 12: 1305–1311
2 Chen Y. Orthopedic applications of gene therapy. J Orthop Sci, 2001, 6: 199–207
3 Rutherford R B, Moalli M, Franceschi R T, et al. Bone morphogenetic protein-transduced human fibroblasts convert to osteoblasts and form bone *in vivo*. Tissue Eng, 2002, 8: 441–452
4 Aviles M O, Lin C H, Zelivyanskaya M, et al. The contribution of plasmid design and release to *in vivo* gene expression following delivery from cationic polymer modified scaffolds. Biomaterials, 2010, 31: 1140–1147
5 Bonadio J, Smiley E, Patil P, et al. Localized, direct plasmid gene delivery *in vivo*: Prolonged therapy results in reproducible tissue regeneration. Nat Med, 1999, 5: 753–759
6 Heo S J, Kim S E, Wei J, et al. Fabrication and characterization of novel nano- and micro-HA/PCL composite scaffolds using a modified rapid prototyping process. J Biomed Mater Res A, 2009, 89A: 108–116
7 Nie H, Wang C H. Fabrication and characterization of PLGA/HAp composite scaffolds for delivery of BMP-2 plasmid DNA. J Control Release, 2007, 120: 111–121
8 Li D, Ye C, Zhu Y, et al. Fabrication of poly(lactide-co-glycolide) scaffold embedded spatially with hydroxyapatite particles on pore walls for bone tissue engineering. Polym Adv Tech, 2011, doi: 10.1002/pat.2066
9 Ouyang H W, Cao T, Zou X H, et al. Mesenchymal stem cell sheets revitalize nonviable dense grafts: Implications for repair of large-bone and tendon defects. Transplantation, 2006, 82: 170–174
10 Miyahara Y, Nagaya N, Kataoka M, et al. Monolayered mesenchymal stem cells repair scarred myocardium after myocardial infarction. Nat Med, 2006, 12: 459–465
11 Iwata T, Yamato M, Tsuchioka H, et al. Periodontal regeneration with multi-layered periodontal ligament-derived cell sheets in a canine model. Biomaterials, 2009, 30: 2716–2723
12 Yu M, Zhou W, Song Y, et al. Development of mesenchymal stem cell-implant complexes by cultured cells sheet enhances osseointegration in type 2 diabetic rat model. Bone, 2011, 49: 387–394
13 Nakamura A, Akahane M, Shigematsu H, et al. Cell sheet transplantation of cultured mesenchymal stem cells enhances bone formation in a rat nonunion model. Bone, 2010, 46: 418–424
14 Ma D, Ren L, Chen F, et al. Reconstruction of rabbit critical-size calvarial defects using autologous bone marrow stromal cell sheets. Ann Plast Surg, 2010, 65: 259–265
15 Ma D, Yao H, Tian W, et al. Enhancing bone formation by transplantation of a scaffold-free tissue-engineered periosteum in a rabbit model. Clin Oral Implants Res, 2011, 22: 1193–1199
16 Abbah S A, Lam C X, Ramruttun K A, et al. Autogenous bone marrow stromal cell sheets-loaded mPCL/TCP scaffolds induced osteogenesis in a porcine model of spinal interbody fusion. Tissue Eng Part A, 2011, 17: 809–817
17 Zou X H, Zhi Y L, Chen X, et al. Mesenchymal stem cell seeded knitted silk sling for the treatment of stress urinary incontinence. Biomaterials, 2010, 31: 4872–4879
18 Hong Y, Song H, Gong Y, et al. Covalently crosslinked chitosan hydrogel: Properties of *in vitro* degradation and chondrocyte encapsulation. Acta Biomater, 2007, 3: 23–31
19 Mao Z W, Ma L, Jiang Y, et al. *N*,*N*,*N*-trimethylchitosan chloride as a gene vector: Synthesis and application. Macromol Biosci, 2007, 7: 855–863
20 Karageorgiou V, Kaplan D. Porosity of 3D biomaterial scaffolds and osteogenesis. Biomaterials, 2005, 26: 5474–5491
21 Pfaffl M W. A new mathematical model for relative quantification in real-time RT-PCR. Nucleic Acids Res, 2001, 29: e45
22 Zong C, Xue D, Yuan W, et al. Reconstruction of rat calvarial defects with human mesenchymal stem cells and osteoblast-like cells in poly-lactic-co-glycolic acid scaffolds. Eur Cell Mater, 2010, 20: 109–120
23 Usas A, Ho A M, Cooper G M, et al. Bone regeneration mediated by BMP4-expressing muscle-derived stem cells is affected by delivery system. Tissue Eng Part A, 2009, 15: 285–293
24 Zhou W, Han C, Song Y, et al. The performance of bone marrow mesenchymal stem cell-implant complexes prepared by cell sheet engineering techniques. Biomaterials, 2010, 31: 3212–3221
25 Datta N, Pham Q P, Sharma U, et al. *In vitro* generated extracellular matrix and fluid shear stress synergistically enhance 3D osteoblastic differentiation. Proc Natl Acad Sci USA, 2006, 103: 2488–2493
26 Kimura Y, Miyazaki N, Hayashi N, et al. Controlled release of bone morphogenetic protein-2 enhances recruitment of osteogenic progenitor cells for *de novo* generation of bone tissue. Tissue Eng Part A, 2010, 16: 1263–1270
27 Lecanda F, Avioli L V, Cheng S L. Regulation of bone matrix protein expression and induction of differentiation of human osteoblasts and human bone marrow stromal cells by bone morphogenetic protein-2. J Cell Biochem, 1997, 67: 386–396
28 Guo R, Xu S, Ma L, et al. Enhanced angiogenesis of gene-activated dermal equivalent for treatment of full thickness incisional wounds in a porcine model. Biomaterials, 2010, 31: 7308–7320
29 Thanou M, Florea B I, Geldof M, et al. Quaternized chitosan oligomers as novel gene delivery vectors in epithelial cell lines. Biomaterials, 2002, 23: 153–159
30 Fang J, Zhu Y Y, Smiley E, et al. Stimulation of new bone formation by direct transfer of osteogenic plasmid genes. Proc Natl Acad Sci USA, 1996, 93: 5753–5758
31 Uchiyama H, Yamato M, Sasaki R, et al. *In vivo* 3D analysis with micro-computed tomography of rat calvaria bone regeneration using periosteal cell sheets fabricated on temperature-responsive culture dishes. J Tissue Eng Regen Med, 2011, 5: 483–490
32 Chew S A, Kretlow J D, Spicer P P, et al. Delivery of plasmid DNA encoding bone morphogenetic protein-2 with a biodegradable branched polycationic polymer in a critical-size rat cranial defect model. Tissue Eng Part A, 2010, 17: 751–763
33 Kasper F K, Young S, Tanahashi K, et al. Evaluation of bone regeneration by DNA release from composites of oligo(poly(ethylene glycol) fumarate) and cationized gelatin microspheres in a critical-sized calvarial defect. J Biomed Mater Res A, 2006, 78: 335–342
34 Govender S, Csimma C, Genant H K, et al. Recombinant human bone morphogenetic protein-2 for treatment of open tibial fractures: A prospective, controlled, randomized study of four hundred and fifty patients. J Bone Joint Surg Am, 2002, 84-A: 2123–2134
35 Glassman S D, Carreon L, Djurasovic M, et al. Posterolateral lumbar spine fusion with INFUSE bone graft. Spine J, 2007, 7: 44–49